Photodegradation of Methyl Orange by V^{5+} and Ho^{3+} Co-doped TiO_2

SHI Jianwen, ZHENG Jingtang, CHEN Jiaoxia, ZHAO Yucui
(The State Key Laboratory of Heavy Oil, China University of Petroleum, Dongying, Shandong 257061, China)

Abstract: The un-doped, single-doped and co-doped TiO_2 nanoparticles have been prepared by sol-gel method and characterized with X-ray diffraction (XRD) and UV-Vis absorption spectra, and their photocatalytic activity have been investigated by photocatalytic oxidation of methyl orange. It is found that V^{5+} doping broadens the absorption profile, improves photo utilization of TiO_2, and then generates more electron-hole pairs; Ho^{3+} doping restrains the increase of grain size, leads to crystal expansion and matrix distortion and retards the recombination of the photoexcited carriers. The photocatalytic activity of TiO_2 co-doped with V^{5+} and Ho^{3+} ions is improved related to the cooperative actions of the two dopants.

Key words: TiO_2; photocatalysis; co-doped; vanadium; holmium
CLC number: TG146 Document code: A Article ID: 0529-6579 (2007) Sl-0011-03

1 Introduction

The photocatalytic oxidation of organic compounds by TiO_2 catalyst has been extensively studied in the past decades[1-2]. But TiO_2 utilizes only a very small fraction of the solar spectrum and the photocatalytic activity is limited by fast photogenerated carriers recombination. In order to improve its photocatalytic activity, co-doped with two kinds of ions have been investigated in recent years[3-4]. In this work, The V^{5+} and Ho^{3+} co-doped TiO_2 was prepared and its photocatalytic activity was evaluated by photodegradation of methyl orange in solution.

2 Experiment

NH_4VO_3 and $Ho(NO_3)_3 \cdot 6H_2O$ were used as precursor of V^{5+} and Ho^{3+}, respectively. Samples were prepared and characterized, and photocatalytic efficiency was tested as described in our earlier publication[5]. For convenience, the samples were labeled as TV(X), TH(Y) for V^{5+} and Ho^{3+} — doped TiO_2, and TV(X)H(Y) for V^{5+} and Ho^{3+} co-doped TiO_2, where X and Y referred to the nominal atomic concentration of V^{5+} and Ho^{3+}, respectively.

3 Results and discussion

3.1 X-ray diffraction

X-ray diffraction patterns (not shown) indicate that all samples prepared have the anatase structure. The average crystal size is calculated from the broadening of the (101) peak of anatase using scherrer's equation, and the distortion of the TiO_2 matrices is also estimated. The results are summarized in Tab. 1. The influence of V^{5+} doping on the crystal size is very unapparent. While the crystal size decreases because of Ho^{3+} doping which implies Ho^{3+} doping restrains the increase of crystalloid. The crystal volume and matrix distortion of doped samples larger than un-doped sample, which indicates matrix may be expanded and distorted.

Tab. 1 XRD analysis result of samples

Doped element	Doped content /%	Crystal size /nm	Matrix distortion /%	Crystal parameter		
				a/nm	c/nm	V/nm³
Un-doped	0	18.2	0.8595	0.3892	0.8084	0.1225
V	1	18.3	0.8548	0.3885	0.8309	0.1254
Ho	1	14.2	1.1000	0.3889	0.8245	0.1247
V/Ho	0.5/0.5	14.5	1.0781	0.3893	0.8270	0.1253

3.2 UV-Vis absorption spectra

Fig. 1 shows the UV-Vis absorption spectra of samples. Compared with the spectrum of pure titania, a tiny blue-shift of the absorption profile in the Ho^{3+} — doped TiO_2, and the red-shift in the V^{5+} — doped TiO_2 are clearly observed. The sample of TV(0.1)H(0.5) shows the same red-shift and the shifted degree is be-

①收稿日期: 2007-01-10
作者简介: 石建稳 (1976年生), 男, 博士研究生; 通讯联系人: 郑经堂; E-mail: shijnwn@163.com

tween of them.

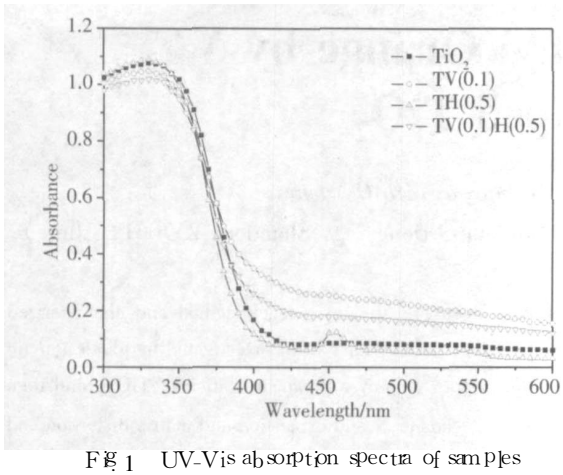

Fig. 1 UV-Vis absorption spectra of samples

3.3 Photocatalytic activity

The evolutions of methyl orange photodegradation are presented in Fig. 2. In comparison with pure TiO_2, doping improves the photocatalytic activity of TiO_2, and co-doping with V^{5+} and $H\partial^{+}$ can enhance the photocatalytic activity more. Such an improvement implies that there is a synergistic effect in catalytic activity when both V^{5+} and $H\partial^{+}$ are co-doped.

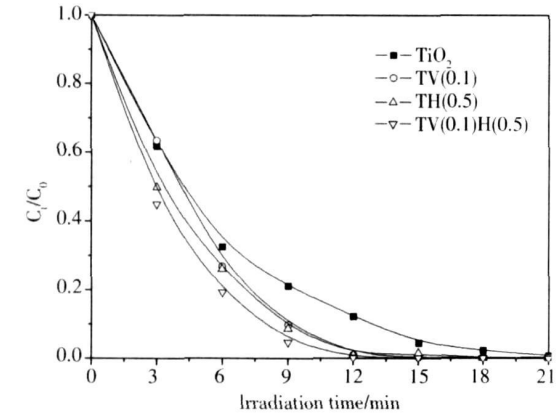

Fig. 2 Degradation curves of methyl orange

V^{5+} doping broadens the absorption profile of TiO_2 (Fig. 1). It shows that V^{5+} doping improves photo utilization of TiO_2. $H\partial^{+}$ doping leads crystal expansion and matrix distortion (Tab. 1). Expansion in crystal matrix creates oxygen vacancies, which generate shallow energy states in the bottom of the conduction band and served as an electron trap sites[6]. So the recombination of photogenerated carriers is prevented effectively. When both V^{5+} and $H\partial^{+}$ are co-doped, a cooperative operation will be produced. V^{5+} doping improves photo utilization of TiO_2 and generates more electron-hole pairs. $H\partial^{+}$ doping leads to crystal expansion and matrix distortion, and retards the recombination of the photoexcited carriers. So the photocatalytic activity of TiO_2 co-doped with V^{5+} and $H\partial^{+}$ is improved.

4 Conclusions

The photocatalytic activity of TiO_2 co-doped with V^{5+} and $H\partial^{+}$ ions can be improved because of the co-operative actions of the two dopants. V^{5+} doping improves photo utilization, and generates more electron-hole pairs. $H\partial^{+}$ doping restrains the recombination of the photoexcited change carriers.

References:

[1] GOU Y Q, CHEN D Y, SU Z X. Photocatalyst of nanometer TiO_2/conjugated polymer complex employed for depigmentation of methyl orange[J]. Applied Catalysis A: General, 2004, 261: 15—18.

[2] TOPALOV A S, SOJIC D V, MOLNAR-GABOR D A, et al. Photocatalytic activity of synthesized nanosized TiO_2 towards the degradation of herbicide mecoprop[J]. Applied Catalysis B: Environmental, 2004, 54: 125—133.

[3] CHEN S Y, TING C C, HSIEH W F. Comparison of visible fluorescence properties between sol-gel derived Er^{3+}-Yb^{3+} and Er^{3+}—Y^{3+} co-doped TiO_2 films[J]. Thin Solid Films, 2003, 434: 171—177.

[4] WEI H Y, WU Y S, LUN N, et al. Preparation and photocatalysis of TiO_2 nanoparticles co-doped with nitrogen and lanthanum[J]. Journal of materials science, 2004, 39: 1305—1308.

[5] SHI J W, ZHENG J T, HU Y, et al. Photodegradation of methyl orange in water on $H\partial^{+}$—doped TiO_2 nanoparticles under ultraviolet irradiation[A]. The progress of green oxidation/reduction technologies[C], Dalian, 2006. 55—58.

[6] Chen J T, Li X J, Yang Y, et al. Effect of RE doping for photocatalytic properties of TiO_2 thin films[J]. Journal of The Chinese Rare Earth Soc, 2003, 21(special): 67—71.

（下转 20页）

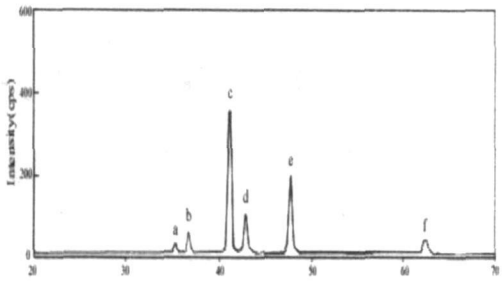

Fig. 1 X-ray diffraction of the product powders

$Li_3Fe_3O_3$ was the primary impurity. However, the amorphous carbon appeared and the size of Fe_4N powders increased along with the increasing of the reaction temperature (> 450 ℃) and reaction time (> 10 h).

3 Conclusions

Nanoparticle Fe_4N was synthesized through benzene-thermal reaction of anhydrous $FeCl_3$ with Li_3N. The optimum condition for the synthesis of nanoparticle Fe_4N was stirred at the temperature range of 450 ~ 500 ℃ for more than 30 h. The average crystalline size of Fe_4N was about 10 nm. The reaction conditions were easy to control.

References:

[1] BAILAR J C, EMELEUS H J, NYHOLM R. Comprehensive Inorganic Chemistry [M]. Oxford: Pergamon Press, 1973. 12.

[2] WANG L J, HAO Z X, YING P L. Preparation and aniline hydrogenation performance of iron nitride catalysts [J]. Chinese J Catal, 1998, 19 (6): 554—558.

[3] ROSS C B, WADE T, CROOKS R M. Electrochemical synthesis of metal nitride ceramic precursors in liquid ammonia electrolyte solutions [J]. Chem Mater, 1991, 3 (5): 768—771.

[4] BONNEAU P R, JARVIS R F, KANER R B. Solid-state metathesis as a quick route to transition-metal mixed dichalcogenides [J]. Inorg Chem, 1990, 31 (11): 2127—2132.

[5] CHEN Y, HALSTEAD T, WILLIAMS J S. Influence of milling temperature and atmosphere on the synthesis of iron nitrides by ball milling [J]. Mater Sci Eng, 1996, 206 (1): 24—29.

[6] YAMAGUCHI T, SAKITA M, NAKAMURA M. Synthesis and characteristics of Fe_4N powders and thin films [J]. J Magn Magn Mater [J], 2000, 215: 529—531.

[7] KOLTYPIN Y, CAO X, PROZOROV R. Sonochemical synthesis of iron nitride nanoparticles [J]. J Mater Chem, 1997, 7 (12): 2453—2456.

苯热法合成环境催化材料纳米氮化铁

殷永泉，刘 翔，郑 艳，崔兆杰

（山东大学环境科学与工程学院，山东 济南 250100）

摘 要：采用苯热法合成环境催化材料纳米氮化铁。在高压反应釜内，无水 $FeCl_3$ 与 Li_3N 在通氮气的苯溶液和 450 ~ 500 ℃条件下反应 30 h，XRD结果表明主要产物为 Fe_4N，晶体的平均直径约为 10 nm，该反应条件容易控制。

关键词：氮化铁；苯热合成；纳米材料；合成

中图分类号：O69，X5

（上接第 12页）

V^{5+}、$H^{\delta+}$ 共掺杂 TiO_2 光降解甲基橙

石建稳，郑经堂，陈姣霞，赵玉翠

（中国石油大学 （华东）重质油国家重点实验室，山东 东营 257061）

摘 要：采用溶胶－凝胶法制备了不掺、单掺和共掺杂纳米 TiO_2，对样品进行了 XRD和 UV-Vis吸收光谱分析，并以甲基橙的光脱色反应考察了样品的光催化性能。结果发现 V^{5+}拓宽了 TiO_2光谱响应范围，提高了光的利用率，产生更多的电子－空穴对；$H^{\delta+}$的掺杂抑制了 TiO_2 粒径的长大，引起了晶格的畸变和膨胀，延缓了光生载流子的复合；V^{5+}、$H^{\delta+}$共掺杂时，由于两种掺杂物的共同作用，可进一步提高 TiO_2 的光催化性能。

关键词：二氧化钛；光催化；共掺杂；钒；钛

中图分类号：TG146